

Multi-particle dispersion in fully developed turbulence

L. Biferale¹, G. Boffetta², A. Celani³, B.J. Devenish¹, A. Lanotte⁴, and F. Toschi⁵

¹ *Dept. of Physics and INFN, University of “Tor Vergata”,
Via della Ricerca Scientifica 1, 00133 Roma, Italy*

² *Dipartimento di Fisica Generale and INFN, Università degli Studi di Torino, Via Pietro Giuria 1, 10125, Torino, Italy
and CNR-ISAC, Sezione di Torino, Corso Fiume 4, 10133 Torino, Italy*

³ *CNRS, INLN, 1361 Route des Lucioles, 06560 Valbonne, France*

⁴ *CNR-ISAC, Sezione di Lecce, Str. Prov. Lecce-Monteroni km. 1.200, 73100 Lecce, Italy*

⁵ *Istituto per le Applicazioni del Calcolo, CNR, Viale del Policlinico 137, 00161 Roma, Italy*

(Dated: August 7, 2018)

The statistical geometry of dispersing Lagrangian clusters of four particles (tetrahedra) is studied by means of high-resolution direct numerical simulations of three-dimensional homogeneous isotropic turbulence. We give the first evidence of a self-similar regime of shape dynamics characterized by almost two-dimensional, strongly elongated geometries. The analysis of four-point velocity-difference statistics and orientation shows that inertial-range eddies typically generate a straining field with a strong extensional component aligned with the elongation direction and weak extensional/compressional components in the orthogonal plane.

PACS numbers: 47.27-i

One of the most characteristic attributes of turbulence is the efficient dispersion and mixing of advected Lagrangian particles [1]. Even though turbulent dispersion bears some similarities to Brownian motion, especially at very large scales and for long times, it has a much richer structure at small scales. This is already visible at the level of single particle dispersion, which is characterized by non-trivial time-correlations of the velocity experienced by the particle along its trajectory (see e.g. [2]). The statistics of pair dispersion display interesting properties as well (see e.g. [3, 4, 5]), yet the complexity of Lagrangian turbulence is particularly evident when looking at the dispersion of three or more particles. This calls for the description of the geometrical properties of Lagrangian dispersion – the “shape” of the particles’ cloud as well as its “size”. The geometrical characterization of dispersion proved extremely important for the understanding of the problem of passive scalar advection [6] and provides the basis for the efficient modelling of the small-scale velocity dynamics itself [7]. Previous studies dealt with two-dimensional flows [8, 9], synthetic flows [10, 11] or three-dimensional turbulence at moderate Reynolds numbers [7, 12, 13]. In this Letter we study multi-particle Lagrangian statistics by means of high resolution direct numerical simulations of three-dimensional Navier-Stokes turbulence. Simulations were done at resolutions of 1024^3 corresponding to a Reynolds number $R_\lambda \sim 280$ (see Ref. [14]). The other parameters of the numerical simulation are as follows: energy dissipation $\varepsilon = 0.81(8)$, viscosity $\nu = 8.8 \cdot 10^{-4}$, Kolmogorov length scale $\eta = 5 \cdot 10^{-3}$, integral scale $L = 3.14$, Lagrangian velocity autocorrelation time $T_L = 1.2$, Kolmogorov time scale $\tau_\eta = 3.3 \cdot 10^{-2}$.

With the present choice of parameters the dissipative range of length scales is exceptionally well resolved. Upon having reached a statistically stationary velocity

field, the Lagrangian tracers were seeded in the flow. Their trajectories were integrated according to

$$\frac{d\mathbf{x}}{dt} = \mathbf{u}(\mathbf{x}(t), t)$$

over a time lapse of the order of a few Lagrangian correlation times, T_L . The velocity field, \mathbf{u} , results from the time-integration of the three-dimensional Navier-Stokes equations (for further details see Ref. [14]).

A set of $3.84 \cdot 10^5$ particles were initially seeded in quadruplets forming $9.6 \cdot 10^4$ regular tetrahedra of the size of the Kolmogorov scale, with centers of mass uniformly distributed over the domain. The evolution of the separations between different particles in each tetrahedron provides a way to quantify the shape evolution. As particles move with the flow the size of the tetrahedra grows in time and their shape deforms, generating a variety of irregular objects. A description of this process is then given in terms of the probability density functions (pdf) of sizes and shapes. Within the inertial range of scales a self-similar evolution of size according to Richardson’s law and a stationary shape distribution are expected. Figure 1 shows a sample of the tetrahedra evolving in the turbulent flow. The presence of very different shapes, from almost regular to very flat and elongated involving the interaction of diverse scales, is evident.

In order to characterize the shape dynamics quantitatively, it is useful to introduce the following change of coordinates [7]: $\boldsymbol{\rho}_0 = (\mathbf{x}_1 + \mathbf{x}_2 + \mathbf{x}_3 + \mathbf{x}_4)/2$, $\boldsymbol{\rho}_1 = (\mathbf{x}_2 - \mathbf{x}_1)/\sqrt{2}$, $\boldsymbol{\rho}_2 = (2\mathbf{x}_3 - \mathbf{x}_2 - \mathbf{x}_1)/\sqrt{6}$, $\boldsymbol{\rho}_3 = (3\mathbf{x}_4 - \mathbf{x}_3 - \mathbf{x}_2 - \mathbf{x}_1)/\sqrt{12}$. By virtue of the statistical homogeneity of the velocity field as well as of the initial distribution of the centers of mass, the Lagrangian statistics do not depend on $\boldsymbol{\rho}_0$. The information about the particle separations can be embodied in the square matrix $\boldsymbol{\rho}$ whose

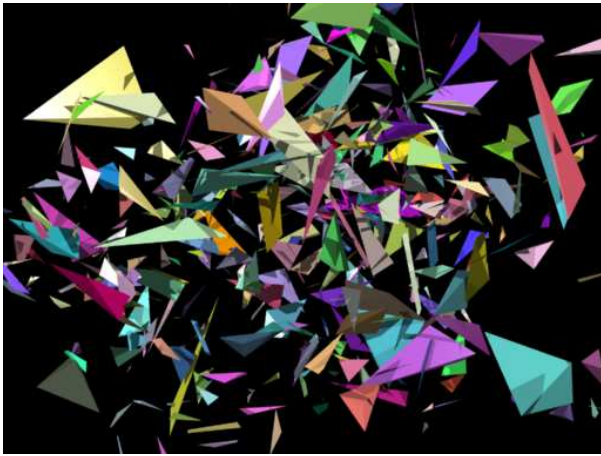


FIG. 1: Snapshot at $t = 0.65T_L$ of 480 tetrahedra evolving in the turbulent flow starting from regular tetrahedra at the Kolmogorov scale.

columns are the three vectors ρ_i with $i = 1, 2, 3$. Denoting by g_i ($g_1 \geq g_2 \geq g_3$) the eigenvalues of the moment of inertia matrix, $\mathbf{I} = \rho\rho^T$ (that is positive defined), we have that the size of the tetrahedron is $r \equiv \sqrt{\text{tr}(\mathbf{I})} = \sqrt{g_1 + g_2 + g_3} = \sqrt{\frac{1}{8} \sum_{i,j} |\mathbf{x}_i - \mathbf{x}_j|^2}$, whereas the volume can be expressed as $V = \frac{1}{3} \det(\rho) = \frac{1}{3} \sqrt{g_1 g_2 g_3}$. A convenient characterization of shapes is given in terms of the dimensionless quantities $I_i = g_i/r^2$ (where obviously $I_1 + I_2 + I_3 = 1$). For a regular tetrahedron one has $I_1 = I_2 = I_3 = 1/3$. If the four points are coplanar one has $I_3 = 0$ and for a collinear configuration $I_2 = I_3 = 0$.

Figure 2 shows the temporal evolution of the mean eigenvalues of $\rho\rho^T$ for the smallest regular tetrahedra with $g_i(0) = \delta x^2/2$. Two very different regimes are evident: at small times $t < \tau_\eta$ the evolution of tetrahedra is governed by the dissipative range of turbulence. Because of the smoothness and incompressibility of the velocity field in this range, the volume of each tetrahedron is approximately preserved and so is its average value which is shown in Fig. 2. In the viscous range the shape dynamics are essentially characterized by the Lagrangian Lyapunov exponents [15]: as a consequence the mean square separation r^2 grows exponentially in time. From the average growth rate of the logarithms of the separations, $R(t) = |\rho_1|$, areas $A(t) = \frac{\sqrt{3}}{2} |\rho_1 \times \rho_2|$ and volumes $V(t) = \frac{1}{3} |\rho_1 \times \rho_2 \cdot \rho_3|$ at small times, we can obtain an estimation of the Lagrangian Lyapunov spectrum as shown in Fig. 2. We found two positive Lyapunov exponents, with $\lambda_1 \tau_\eta \simeq 0.12$ and $\lambda_2 \simeq \lambda_1/4$, in agreement with previous findings at lower R_λ [16, 17]. The sum of the three Lyapunov exponents so obtained is close to zero for times up to $3\tau_\eta$.

The exponential growth brings particle separations outside the dissipative range, where the velocity field becomes rough and the inertial range sets in. According to

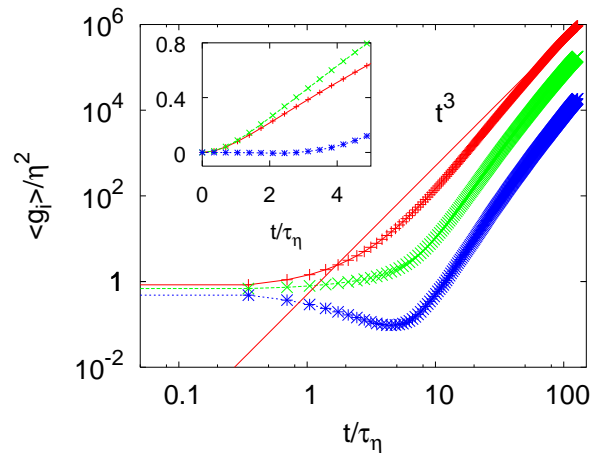


FIG. 2: Evolution of the mean eigenvalues g_1 (+), g_2 (\times) and g_3 ($*$) of the moment of inertia matrix $\mathbf{I} = \rho\rho^T$. The line represents the dimensional scaling t^3 . In the inset, from top to bottom: evolution at small times of $\langle \ln A(t) \rangle$ (surface), $\langle \ln R(t) \rangle$ (distance), $\langle \ln V(t) \rangle$ (volume). The linear slopes of the three curves in the range of times $\tau_\eta < t < 3\tau_\eta$ yield $\lambda_1 + \lambda_2$, λ_1 and $\lambda_1 + \lambda_2 + \lambda_3$, respectively.

the Kolmogorov-Richardson scaling, eigenvalues should grow as $g_i \sim t^3$. As previously reported [7], it is hard to extract a clear scaling regime for the shape dynamics shown in Fig. 2. The main reason for the lack of self-similarity is due to the contamination of the inertial range by the dissipative range. Indeed, because of the strong shape distortion taking place at the crossover between the dissipative and inertial ranges (as shown in Fig. 2 by the separation of the three eigenvalues), a significant fraction of tetrahedra has one side in the dissipative range even at times much larger than τ_η . In order to overcome this problem we have utilized the technique of doubling time statistics that has already been successfully used to remove contaminations in the statistics of pair dispersion [4, 5, 18]. Here, we focus on the doubling times of the eigenvalues g_i : we compute the times, $T(g_i)$, taken by a tetrahedron to increase its value of g_i by a factor a . The result is shown in Fig. 3. The presence of a scaling range $T \sim g^{1/3}$ is more clear and the self-similarity is made evident by superimposing the three curves on top of each other by a simple multiplicative factor on the g -axis. The ratio of the three eigenvalues in the scaling range is $g_1 : g_2 : g_3 = 40 : 8 : 1$, corresponding to shape indices $I_2 \approx 0.16$ and $I_3 \approx 0.02$. The presence of a range where the doubling times for different eigenvalues are the same is equivalent to stating that the typical shape of the tetrahedron is preserved while its size increases according to Richardson's law.

In view of the existence of a self-similar regime for shape evolution, one would expect that the statistics of the shape indices, I_i , should reach a time-independent distribution. However, a direct inspection of the data

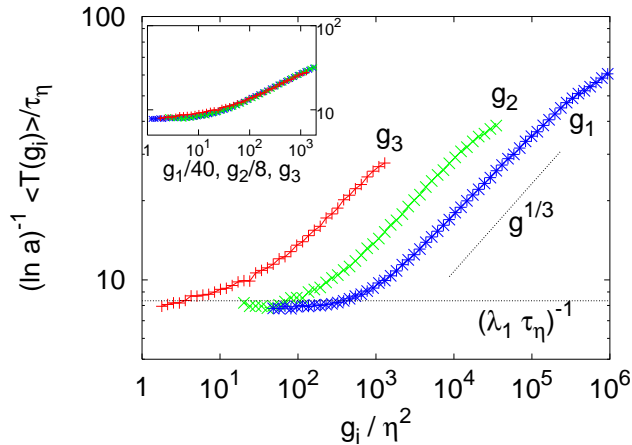


FIG. 3: Doubling times for the eigenvalues, g_i , of the moment of inertia matrix, $\rho\rho^T$. In the inset: the same data rescaled on the horizontal axis with the proportions $g_1 : g_2 : g_3 = 40 : 8 : 1$

does not support this conclusion (not shown here, the results do not present an appreciable scaling range in time in spite of the relatively high R_λ as compared with Ref. [7]). Once more this lack of a scaling range in the time domain can be traced back to the contamination by the dissipative range dynamics.

This difficulty can be overcome by selecting those tetrahedra with eigenvalues in the ranges $5 \cdot 10^2 \eta^2 < g_1 < 5 \cdot 10^5 \eta^2$, $5 \cdot 10^1 \eta^2 < g_2 < 5 \cdot 10^4 \eta^2$, $5 \cdot \eta^2 < g_3 < 5 \cdot 10^3 \eta^2$. The thresholds are obtained by identifying the scaling ranges in Fig. 3. This procedure removes about 60% of the initial tetrahedra, mostly because g_3 falls below its lower threshold. The probability density functions of the shape indices I_2 , I_3 after the selection are shown in Fig. 4. The existence of an invariant regime appears now very clearly. In this regime, the normalised probability density functions at different times collapse, and the mean values hence display a plateau in time: for the third index, the mean value $\langle I_3 \rangle \simeq 0.011 \pm 0.001$ is not too far from the Gaussian value 0.03, while the second index is concentrated on values much smaller ($\langle I_2 \rangle \simeq 0.135 \pm 0.003$ as opposed to 0.22). Those values indicate a relative abundance of flat and elongated configurations. The tendency to form almost two-dimensional structures has mostly an “entropic” origin: indeed there is a large number of pancake-like tetrahedra (very small I_3) already for Gaussian, independent particle positions, as shown by the corresponding distribution in Fig. 4. However, it has to be remarked that the pdf of I_3 is significantly more peaked at small values than the Gaussian one. The preference for elongated structures ($I_2 \ll I_1$) has a clear dynamical origin, since it has no equivalent in the Gaussian ensemble.

An interesting issue that we do not address here is connected with the possibility of subleading, anomalous

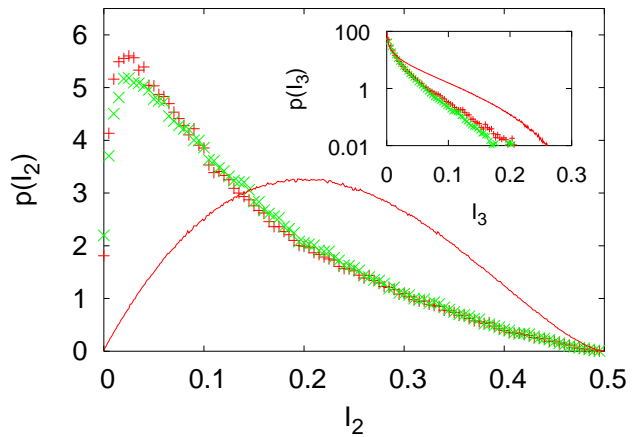


FIG. 4: Probability density function of shape indices I_2 and I_3 (inset) at times $t = 35\tau_\eta$ (+) and $t = 63\tau_\eta$ (×). The full lines are the pdfs for independent, Gaussian distributed particle positions.

scaling in the tetrahedra distribution. In the simpler case of particles advected by a Gaussian and white-in-time velocity field, it is known that the asymptotic behaviour of the multi-particle pdf, when the initial points are close, is governed by an expansion in zero modes and slow modes of a given evolution operator [6]. There, anomalous corrections emerge as sub-leading terms to the Richardson scaling. These corrections are connected to the anomalous scaling of the structure functions of a passive scalar field advected by the flow. Here, in the presence of a real turbulent flow, one can only argue that similar properties may still hold [8]. In order to check this, one should perform a delicate compensation between the evolution of the pdf with different initial tetrahedra shapes, in order to cancel the leading scaling terms and to highlight the sub-leading contributions.

The dynamics of the shape evolution can be elucidated by analyzing the local geometrical properties of Lagrangian velocities. In analogy with the relative coordinates ρ , we introduce the relative velocity matrix \mathbf{W} : $\mathbf{W}_1 = (\mathbf{u}_2 - \mathbf{u}_1)/\sqrt{2}$, $\mathbf{W}_2 = (2\mathbf{u}_3 - \mathbf{u}_2 - \mathbf{u}_1)/\sqrt{6}$, $\mathbf{W}_3 = (3\mathbf{u}_4 - \mathbf{u}_3 - \mathbf{u}_2 - \mathbf{u}_1)/\sqrt{12}$. Obviously, $\dot{\rho} = \mathbf{W}$. The geometrical aspects of Lagrangian velocity evolution can be described by the tetrahedron “turbulent diffusion” tensor

$$\mathbf{K} \equiv \frac{1}{2} \frac{d}{dt} \rho \rho^T = \frac{1}{2} (\mathbf{W} \rho^T + \rho \mathbf{W}^T). \quad (1)$$

The trace $tr(\mathbf{K}) = \frac{1}{8} \sum_{i,j} (\mathbf{u}_i - \mathbf{u}_j) \cdot (\mathbf{x}_i - \mathbf{x}_j)$ is proportional to the longitudinal velocity difference multiplied by the separation averaged over all pairs within the tetrahedron. The geometrical information about the Lagrangian velocity fluctuations may be obtained from the eigenvalues $\kappa_1 \geq \kappa_2 \geq \kappa_3$ of \mathbf{K} which are shown in Fig. 5. On dimensional grounds these should grow in time as t^2 or,

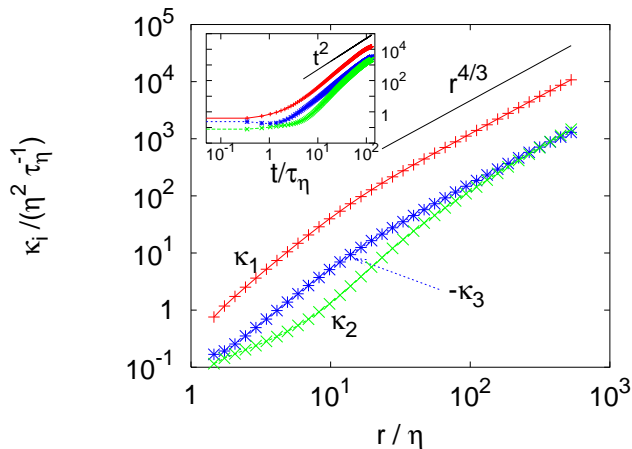


FIG. 5: Evolution of the mean eigenvalues of the “turbulent diffusion tensor”, \mathbf{K} , as a function of the tetrahedron size, r . In the inset, the eigenvalues as a function of time.

equivalently, with the tetrahedron size, r , as $r^{4/3}$: this is satisfied to a good accuracy for all three eigenvalues, especially as a function of size. The third eigenvalue, κ_3 , is negative (notice that, strictly speaking, this makes abusive the definition of \mathbf{K} as a diffusion tensor): geometrically this means that the local velocity field experienced by the tetrahedron has two extensional components, a strong one and a weak one, $\kappa_1 \gg \kappa_2$, with the latter smaller by a factor of ten than the former, and a weak compressional component $|\kappa_3| \approx \kappa_2$. It is also interesting to study the relative orientation of the eigenvectors of the matrix $\mathbf{I} = \rho\rho^T$, i.e. the principal axes of inertia, and the eigenvectors of the matrix \mathbf{K} . We found that the directions of the eigenvectors associated with g_1 and κ_1 are preferentially aligned. About 45% of the tetrahedra show a relative angle smaller than $\pi/6$ (for a uniform distribution on a unit sphere one would have 13%). This agrees with the intuitive idea that strongly extensional velocity differences result in intense elongations approximately in the same direction. In the plane orthogonal to the first principal axis of inertia, the eigenvectors of \mathbf{I} and \mathbf{K} associated with the smaller eigenvalues are also aligned albeit to a lesser degree (about 25% of relative angles below $\pi/6$).

The overall geometrical picture that emerges is the following: tetrahedra tend to be elongated, almost coplanar objects, subject to a straining velocity field that has a strong extensional part in the direction of elongation and relatively weak compressive and extensional contributions in the orthogonal plane of approximately equal magnitude. The recent advances in experimental techniques for particle tracking should soon allow precise measurements of shape dynamics in real turbulent

flows. The joint effort on the numerical and experimental side can shed further light on the geometrical statistics of Lagrangian turbulence. This, in turn, will lead to the development of new, more effective parameterizations of small-scale turbulence, a problem of paramount importance for geophysical and industrial applications.

We are grateful to A. Pumir for discussions and useful suggestions. The simulations were performed on the IBM-SP4 of the Cineca (Bologna, Italy). We are grateful to C. Cavazzoni and G. Erbacci for resource allocation and precious technical assistance.

-
- [1] A. S. Monin and A. M. Yaglom, *Statistical Fluid Mechanics* (MIT Press, Cambridge, MA 1975), vol 2.
 - [2] N. Mordant *et al.*, Phys. Rev. Lett. **87**, 214501 (2001). L. Chevillard *et al.*, Phys. Rev. Lett. **91**, 214502 (2003). L. Biferale *et al.*, Phys. Rev. Lett. **93**, 064502 (2004).
 - [3] P.K. Yeung, Phys. Fluids **6**, 3416 (1994). S. Ott and J. Mann, J. Fluid Mech. **422**, 207 (2000). T. Ishihara and Y. Kaneda, Phys. Fluids **14**, L69 (2002). G. Boffetta and I.M. Sokolov, Phys Fluids **14**, 3224 (2002). P.K. Yeung and M.S. Borgas, J. Fluid Mech. **503**, 93 (2004).
 - [4] G. Boffetta and I.M. Sokolov, Phys. Rev. Lett. **88**, 094501 (2002).
 - [5] L. Biferale *et al.*, submitted to Phys. Fluids, arxiv.org/0501054.
 - [6] G. Falkovich, K. Gawędzki, and M. Vergassola, Rev. Mod. Phys. **73**, 913 (2001).
 - [7] M. Chertkov, A. Pumir and B.I. Shraiman, Phys. Fluids **11**, 2394 (1999), A. Pumir, B.I. Shraiman and M. Chertkov, Phys. Rev. Lett. **85**, 5324 (2000), A. Pumir, B.I. Shraiman and M. Chertkov, Europhys. Lett. **56**, 379 (2001), A. Pumir and B. Shraiman, J. Stat. Phys. **113**, 693 (2003).
 - [8] A. Celani and M. Vergassola, Phys. Rev. Lett. **86**, 424 (2001).
 - [9] P. Castiglione and A. Pumir, Phys. Rev. E **64**, 056303 (2001).
 - [10] U. Frisch, A. Mazzino and M. Vergassola, Phys. Rev. Lett. **80**, 5532 (1998).
 - [11] K.A.I. Khan, A. Pumir and J.C. Vassilicos, Phys. Rev. E **68**, 026313 (2003).
 - [12] M.S. Borgas, Proc. 13th Australian Fluid Mech. Conf., Melbourne, (1998).
 - [13] P.K. Yeung *et al.*, IUTAM Symp. Reynolds Number Scaling in Turb. Flow, Princeton, (2002).
 - [14] L. Biferale *et al.*, Phys. Fluids **17**, 021701 (2005).
 - [15] M. Falcioni, G. Paladin and A. Vulpiani, Riv. Nuovo Cimento **14**, 1 (1991).
 - [16] S.S. Girimaji and S. B. Pope, J. Fluid. Mech. **220**, 427 (1990).
 - [17] G. Falkovich and A. Pumir, Phys. Fluids **16**, L47 (2004).
 - [18] V. Artale, G. Boffetta, A. Celani, M. Cencini and A. Vulpiani, Phys. Fluids **9** 3162 (1997).